Int J Clin Exp Med 2016;9(2):753-759
www.ijcem.com /ISSN:1940-5901/IJCEM0016946

Original Article

Breast cancer imaging with fluoresce in isothiocyanate-modified gold nanoparticles *in-vitro* and *in-vivo*

Guanghua Yang, Sen Xiang, Kaifang Zhang, Dongdong Gao, Chen Zeng, Fuli Zhao

Department of Medical Oncology, Zhumadian Central Hospital, Zhumadian 463000, Henan Province, China

Received September 26, 2015; Accepted December 8, 2015; Epub February 15, 2016; Published February 29, 2016

Abstract: Objective: To prepare fluorescein isothiocyanate (FITC)-modified gold nanoparticles (FITC-Au NPs) and conduct *in-vitro* and *in-vivo* breast cancer imaging studies with them. Methods: Nanosizer and transmission electron microscopy were used to characterize the diameter and morphology of FITC-Au NPs and their stability; UV spectrophotometer and fluorescence spectrometer were used to detect the UV and fluorescence spectra of FITC-Au NPs; Cell counting kit (CCK-8) method was used to detect the *in-vitro* cytotoxicity of Au NPs and FITC-Au NPs in breast cancer 4T1 cells; Confocal microscopy was used to observe FITC-Au NPs uptaken by cells; A small living animals fluorescence imaging system, after tail intravenous injection, was used to observe the distribution of FITC-Au NPs in tumor-bearing mice and the concentration of NPs in the tumor region. Results: The average diameter of Au NPs and FITC-Au NPs were 43 nm and 52.6 nm, respectively. FITC-Au NPs were globular nanoparticles. After standing for 28 days, NPs and FITC-Au NPs showed no change in diameter. The UV spectra of FITC-Au NPs showed a characteristic absorption peak of FITC and Au NP, and the maximal emission peak of FITC-Au NP (520 nm) was excited by 488 nm laser. No significant cytotoxicity was found for cells treated by 0-150 ug/ml of Au NPs and FITC-Au NPs for 12 or 24 hours. Compared with free FITC, FITC-Au NP were uptaken by cells remarkably. In addition, results of *in-vivo* study indicated that FITC-Au NPs passively targeted the tumor region efficiently. Conclusion: FITC-Au NPs can be applied as the contrast agent of *in-vivo* and *in-vitro* breast cancer fluorescence imaging, providing a molecular imaging basis for the medical diagnosis of breast cancer.

Keywords: Gold nanoparticle, isothiocyanate, fluorescence imaging, tumor imaging and diagnosis

Introduction

Breast cancer is one of the major diseases affecting women's health. It is reported that its incidence ranks first among malignant tumors in women across the world [1, 2]. For the treatment of malignant tumors, early diagnosis, periodic monitoring and timely treatment are crucial [3, 4]. In recent years, the diagnosis, monitoring and treatment of tumors have developed rapidly. However, there are still problems, such as low resolution of diagnostic techniques [5, 6]. Therefore, it is vital to find out an effective diagnostic method.

Nanogold is a member of nano material family. It has such special physical and chemical properties as super-large specific surface area and physical absorption ability. Because of its monodispersity and good biocompatibility without toxicity or accumulation when used as molecular or drug carriers, it is very promising in the diagnosis, monitoring and treatment of tumor [7-9]. Besides, as a new contrast agent, nanogold is of great potential in the diagnosis and monitoring of tumor [10-12].

In this study, taking advantage of the surface adsorption ability of nanogold, we obtained fluorescent gold nanoparticles by attaching nanogold to isothiocyanate, a commonly used near-infrared fluorescent dye. It was reported that gold nanoparticles as carriers were of good passive tumor-targeting properties due to the high permeability and enhanced permeation and retention (EPR) of solid tumor [13-15]. Therefore, *in-vitro* and *in-vivo* breast cancer imaging was conducted by utilizing the fluorescent gold nanoparticles prepared and fluorescence imaging system, which provided a new

approach for the diagnosis of breast cancer and a new contrast agent for its imaging.

Materials and methods

Experimental materials and instruments

Gold nanoparticles (article No.: NS-40-50) was purchased from NanoSeedz (Hong Kong), isosulfocyanide (FITC) and phenylindole (DAPI) from Sigma (the U.S.), RPMI1640 cell culture medium and fetal calf serum from Gibco (the U.S.), cell counting kit from Dojindo (Japan), nanosizer Zetersizer Nano ZS from Malvern (England), transmission electron microscope LVEM25 from DELONG (the U.S.), UV/Vis./NIR Spectrophotometer V-700 from JASCO (Japan), fluorescence spectrophotometer S1 Sorter from Bruker (the U.S.), confocal microscopy system Leica FCM1000 from Leica (German) and small living animal fluorescence imaging system Maestro from CRi Maestro (the U.S.).

Synthesis of FITC-Au NPs

FITC was dissolved in DMSO, getting 1 mg/ml solution, which was added into 0.5 mg/ml Au NP aqueous solution and was stirred slowly overnight under 4°C. The mixture was then centrifuged with a 30 KD a centrifugal ultra filter under a centrifugal force of 6000 g for 30 min. Afterwards, it was dialyzed with an activated dialysis bag until excessive FITC molecules were removed. The purified FITC-Au NP solution was stored in a refrigerator at 4°C.

Characterization of FITC-Au NPs

The average diameter of Au NPs and FITC-Au NPs were measured with a nano-particle size analyzer. The morphology of FITC-Au NPs was observed by transmission electron microscopy. Their UV and fluorescence spectra of FITC, Au NPs and FITC-Au NPs were detected with a UV/Vis/NIR spectrophotometer and fluorescence spectrophotometer, respectively.

Cytotoxicity test of Au NPs and FITC-Au NPs

Mice breast cancer cells 4T1 from the cell bank of Shanghai Institutes for Biological Sciences (CAS) were cultivated in a incubator with RPMI-1640 medium (including 0% fetal calf serum and 1% penicillin-streptomycin) and 5% CO_2 at 37°C.

Cell suspension (density: 10^5 cells/ml) was prepared by using cells in logarithmic growth phase and cultured in a 96-well cell culture plate (4 wells per group, 100 ul per well) for 24 hours. Then, the old culture solution was discarded and cells were treated with 0-150 ug/ml Au NPs and FITC-Au NP for 12 and 24 hours, respectively. This culture solution was discarded again and a new one with 10% CCK-8 reagent was added to incubate for 30 min. Finally, the resultant mixture was detected for the absorbance at 450 nm (A450) with a microplate reader. The bigger the A450, the larger the cell viability.

Cell imaging test by confocal microscopy

Cell suspension (density: 10^5 cells/ml) was prepared by using cells in logarithmic growth phase and cultured in a confocal dish until cell adherence was observed. After that, the old culture solution was removed and a new one with 30 ug/ml FITC-Au NPs was added. After culturing for 3 hours, the cells were rinsed with PBS for 3 times. At last, an appropriate amount of PBS was added and the mixture obtained was observed under a confocal microscope.

Small mice fluorescence imaging test in-vivo

Female BALB/c nude mice (SPF) were purchased from Vital River Laboratory Animal Technology Co. Ltd. (Beijing). The subcutaneous transplantation tumor model of human breast cancer in mice was established according to the following steps: 150 ul cell suspension (c.a. 10^6 cells) was injected subcutaneously in the back; After disinfection, the mice were raised in animal houses again; About 7 to 10 days' later, when the tumor volume was found to be up to 100 mm^3, FITC and FITC-Au NPs were injected into tumor-bearing mice through caudal vein. Moreover, mice imaging test was conducted by a whole-body fluorescent imaging system pre-injection and 0.1, 1, 2, 6, 12, 24 and 48 hours after injection, and a statistical analysis of fluorescence around the tumor region was performed (7 mice per group).

Statistical analysis

Statistical data was expressed by mean ± S.D. Comparison between groups was conducted by independent sample t test. Statistical analysis was performed by a statistical software

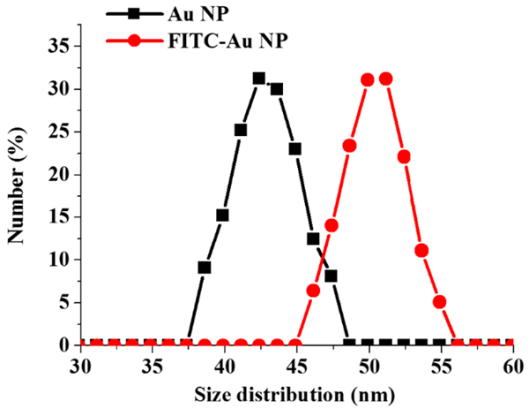

Figure 1. The diameter distribution of Au NPs and FITC-Au NPs.

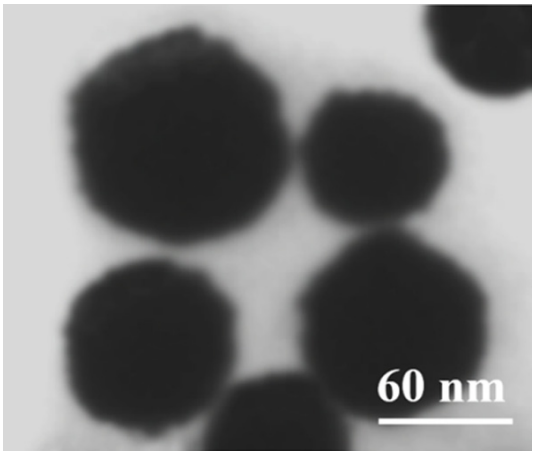

Figure 2. The TEM image of FITC-Au NPs.

SPSS17.0. P<0.05 means the result was statistically significant.

Results

Characterization of FITC-Au NPs

As shown in **Figure 1**, the average diameter of Au NPs was about 43 nm. After attaching to FITC, the diameter increased to 52.6 nm, indicating that FITC was attached to the surface of Au NPs. Electron microscopy (**Figure 2**) suggested that FITC-Au NPs were globular nanoparticles. As shown in **Figure 3**, the diameter almost had no obvious change after Au NPs and FITC-Au NPs solutions stood for 28 days.

Spectrum test of FITC-Au NPs

As shown in **Figure 4**, FITC had a characteristic absorption peak at 480 nm and Au NP had one

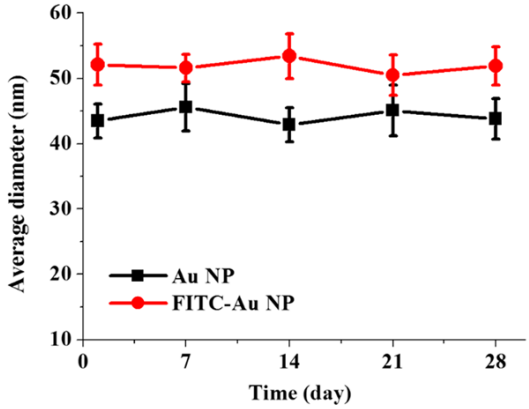

Figure 3. The stability test of FITC-Au NPs.

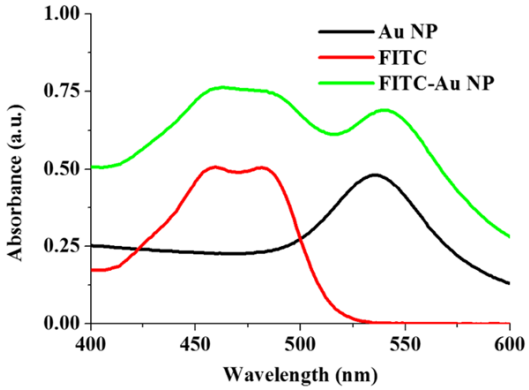

Figure 4. Detection of UV absorption spectrum.

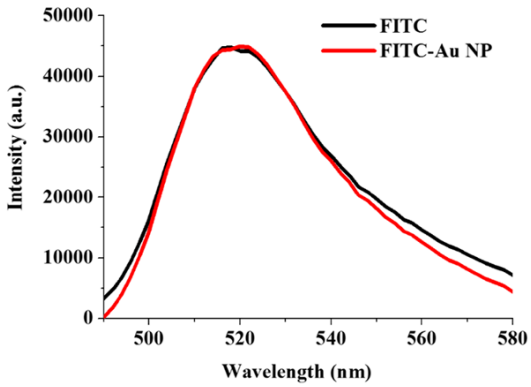

Figure 5. Detection of fluorescence spectrum.

at 534 nm. Besides, FITC-Au NP had strong absorption peaks both at 480 nm and 534 nm, suggesting that FITC was attached to the surface of Au NP successfully. As shown in **Figure 5**, the maximal emission peak was found at 518 nm when FITC was excited by 488 nm laser. Further, the maximal emission peak was

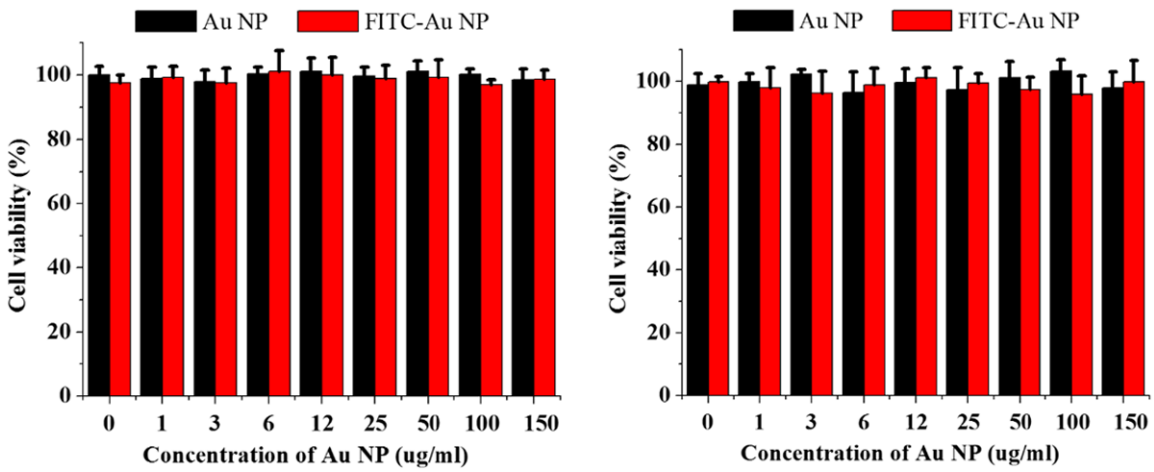

Figure 6. The impact of FITC-Au NP on cell viability.

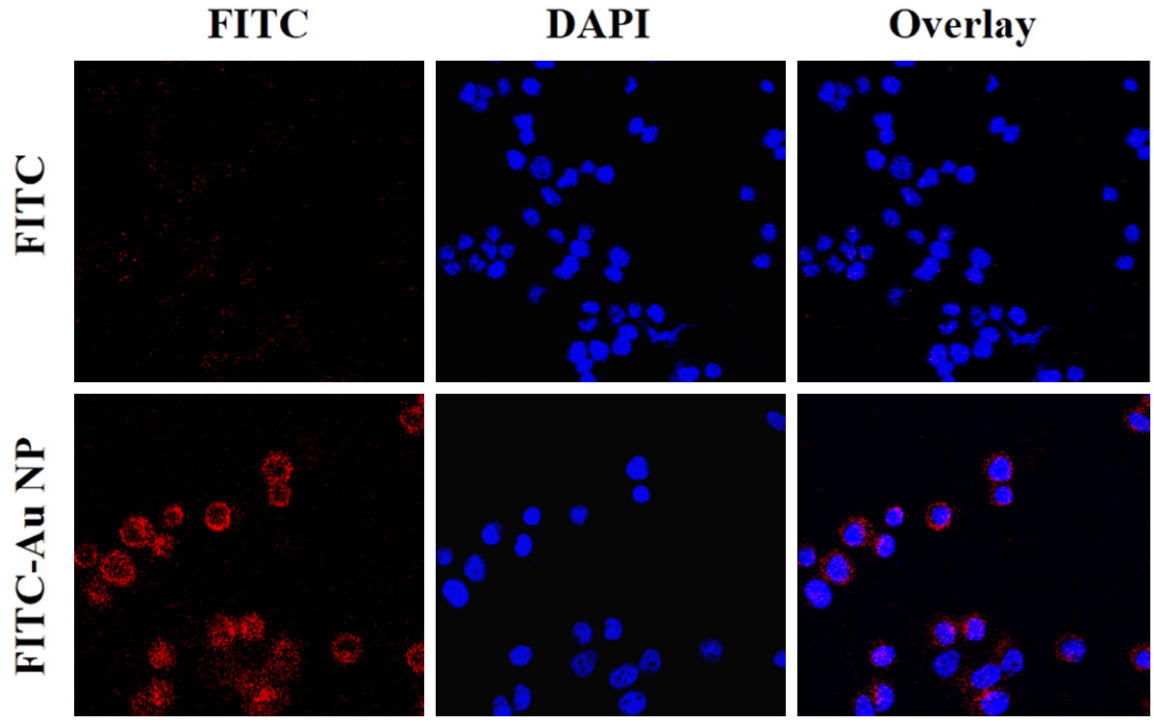

Figure 7. The cell uptake of FITC-Au NP.

still found at 518 nm when FITC was attached to the surface of Au NP, indicating the fluorescent property of FITC-Au NP.

Cytotoxicity test of FITC-Au NP

After cells were treated with 0-150 ug/ml Au NP and FITC-Au NP for 12 and 24 hours, respectively, CCK-8 test results showed that Au NP and FITC-Au NP had no obvious impact on cell viability. It demonstrated that fluorescent reagent based on Au NP almost had no cytotoxicity (as shown in **Figure 6A** and **6B**).

Cell uptake of FITC-Au NP

FITC and FITC-Au NP were incubated with cells for 3 hours, respectively. Then, fluorescence signal within cells was observed by confocal microscopy. As shown in **Figure 7**, the fluores-

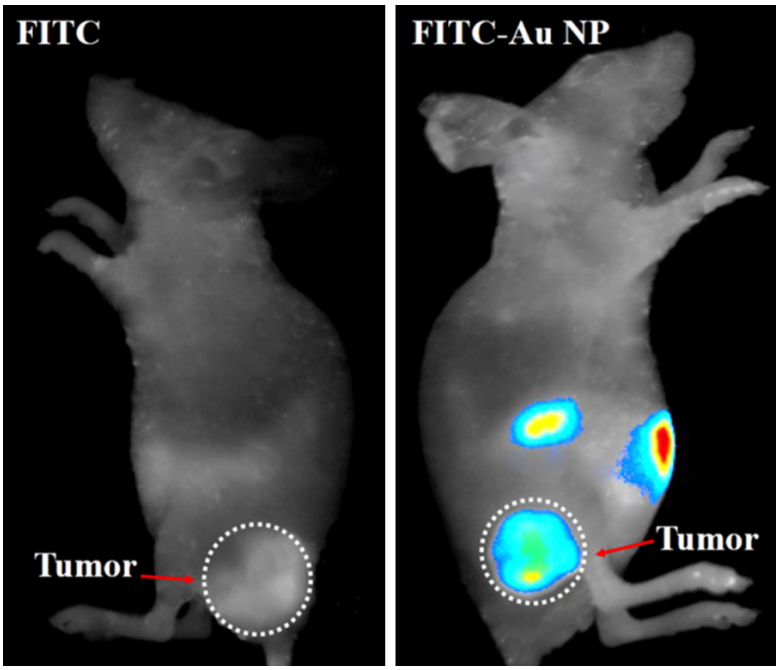

Figure 8. The *in-vivo* fluorescence imaging 24 hours after injection of FITC-Au NP.

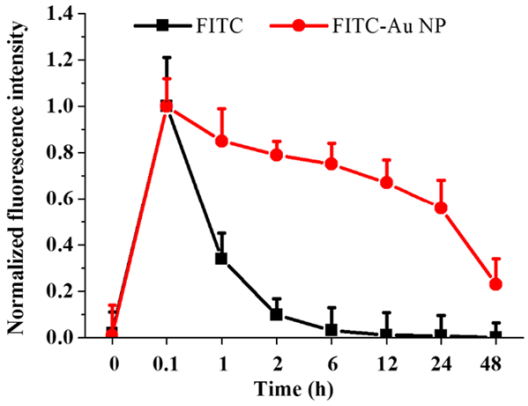

Figure 9. The statistical results of fluorescence signal in tumor region at different time points (n=7).

cence signal in cells treated by FITC in control group was very weak, while the fluorescence signal in cells treated by FITC-Au NP was extremely strong, suggesting a large amount of FITC-Au NP entered into cells.

Whole-body fluorescence imaging

FITC and FITC-Au NP solutions were injected into mice through caudal vein. Then, mice fluorescence imaging was conducted at different time points and the results were presented in **Figure 8**. 24 hours after injection, almost no fluorescence signal was found within mice in FITC group, while significant fluorescence signal was found in tumor region within mice in FITC-Au NP group. It indicated that FITC-Au NP could gather in tumor region, while FITC was readily to be metabolized and removed. **Figure 9** showed statistical results of fluorescence signal within tumor region at different time points. FITC was almost completely metabolized 6 hours after entering into mice, while FITC-Au NP could gather in tumor region for a long time.

Discussion

Functionalized medical nanomaterials, as an emerging field, advanced rapidly in recent years, especially in the treatment and diagnosis of tumor [16, 17], such as nanoliposomes, glairin, carbon nanomaterials and gold nanoparticles [18-20]. Because of their special physical and chemical properties, some functional molecules could be modified on their surface. For example, graphene oxide could be used to carry anti-cancer drug adriamycin. It was of great inhibitory effect on tumor [21]. Further, fluorescent molecules coated by nanoliposomes and modified by targeting molecules on the surface could be used as an active targeting and imaging contrast agent [22]. In this study, gold nanoparticles were used to attach fluorescent molecule FITC for passive targeting for fluorescence imaging of subcutaneous breast cancer. Results suggested that FITC-Au NP had better passive targeting properties and fluorescent imaging effect compared with FITC.

FITC is a fat-soluble small-molecule fluorescent dye. Once entering into body, it is easily to be eliminated and can hardly be gathered in tumor region for imaging [23-25]. Besides, the growth rate of tumor cells is very fast, while that of vascular endothelial cell is slow. A large amount of broken blood vessels presented in tumor. When particles of special sizes get through tumor vessels, they would leak from blood vessels. Hence, it is difficult for FITC to stay. By contrast,

gold nanoparticles, due to the size and EPR effect in solid tumor, will remain in the tumor region for a longer period [26]. Thus, the blood half-life of fluorescent dyes is increased and they can be better used for *in-vivo* fluorescent imaging.

To sum up, FITC-Au NP prepared in this study has good *in-vivo* and *in-vitro* passive targeting property and fluorescent imaging effect on breast cancer cell, providing a new contrast agent and thought for the medical imaging and diagnosis of breast cancer.

Disclosure of conflict of interest

None.

Address correspondence to: Guanghua Yang, Department of Medical Oncology, Zhumadian Central Hospital, Zhumadian 463000, Henan Province, China. E-mail: yangguanghuazmd@163.com

References

[1] Xu L, Xu X, Cheng P. Treatment effect research on gastric tumor by cancer cell vaccine modified with Curcumol. J Pract Oncol 2007; 2: 007.

[2] Qian Y, Kang J, Wen T, et al. Content determination of kaempferol in kaempferol gastric floating sustained-release tablets by HPLC. China Pharmacy 2010; 41: 032.

[3] Lin H, Li X. L1210 cell apoptosis induced by curcumenol. China Pharmacy 2008; 30: 007.

[4] Al-Hajj M, Wicha MS, Benito-Hernandez A, Morrison SJ, Clarke MF. Prospective identification of tumorigenic breast cancer cells. Proc Natl Acad Sci U S A 2003; 100: 3983-3988.

[5] Niu Z, Dong H, Zhu B, Li J, Hng HH, Zhou W, Chen X, Xie S. Highly stretchable, integrated supercapacitors based on single-walled carbon nanotube films with continuous reticulate architecture. Adv Mater 2013; 25: 1058-1064.

[6] Hashida Y, Tanaka H, Zhou S, Kawakami S, Yamashita F, Murakami T, Umeyama T, Imahori H, Hashida M. Photothermal ablation of tumor cells using a single-walled carbon nanotube-peptide composite. J Control Release 2014; 173: 59-66.

[7] Jang K, Eom K, Lee G, et al. Water-stable single-walled carbon nanotubes coated by pyrenyl polyethylene glycol for fluorescence imaging and photothermal therapy. Biochip Journal 2012; 6: 396-403.

[8] Kosuge H, Sherlock SP, Kitagawa T, Dash R, Robinson JT, Dai H, McConnell MV. Near infrared imaging and photothermal ablation of vascular inflammation using single-walled carbon nanotubes. J Am Heart Assoc 2012; 1: e002568.

[9] Yurgel VC, Campos VF, Collares T, et al. Applications of Carbon Nanotubes in Oncology, NanoCarbon 2011 Springer Berlin Heidelberg, 2013.

[10] Mann AP, Bhavane RC, Somasunderam A, Liz Montalvo-Ortiz B, Ghaghada KB, Volk D, Nieves-Alicea R, Suh KS, Ferrari M, Annapragada A, Gorenstein DG, Tanaka T. Thioaptamer conjugated liposomes for tumor vasculature targeting. Oncotarget 2011; 2: 298-304.

[11] Tan LH, Bate J, Mcnamara K, Carmichael AR. Outcome of surgically treated octogenarians with breast cancer. J Postgrad Med 2014; 60: 248-253.

[12] Vecitis CD, Zodrow KR, Kang S, Elimelech M. Electronic-structure-dependent bacterial cytotoxicity of single-walled carbon nanotubes. Acs Nano 2010; 4: 5471-9.

[13] Li R, Zou H, Xiao H, Wu R. Carbon nanotubes as intracellular carriers for multidrug resistant cells studied by capillary electrophoresis-laser-induced fluorescence. Methods Mol Biol 2010; 625: 153-68.

[14] Iyer AK, Khaled G, Fang J, Maeda H. Exploiting the enhanced permeability and retention effect for tumor targeting. Drug Discov Today 2006; 11: 812-818.

[15] Mozafari MR, Khosravi-Darani K, Borazan GG, et al. Encapsulation of food ingredients using nanoliposome technology. International Journal of Food Properties 2008; 11: 833-844.

[16] O'Donnell MR, Abboud CN, Altman J, Appelbaum FR, Arber DA, Attar E, Borate U, Coutre SE, Damon LE, Goorha S, Lancet J, Maness LJ, Marcucci G, Millenson MM, Moore JO, Ravandi F, Shami PJ, Smith BD, Stone RM, Strickland SA, Tallman MS, Wang ES, Naganuma M, Gregory KM. Acute myeloid leukemia. J Natl Compr Canc Netw 2012; 10: 984-1021.

[17] Li SG, Ye ZY. Pharmacological activity effect of andrographolide. Chin Arch Tradit Chin Med 2008; 26: 984-986.

[18] Joshi LS, Pawar HA. Herbal cosmetics and cosmeceuticals: An overview. Nat Prod Chem Res 2015; 3: 2-6.

[19] Tang Y, Li X. Inhibitory effects of zedoray rhizome abstracts on hepatic cell line hepg2 and their mechanisms. Chin Pharmacol Bull 2007; 23: 790-795.

[20] Xu L, Bu P, Xu X. Experimental therapeutic effect of tumor cell vaccine constructed by curcumol on gastric cancer. Journal of Traditional Chinese Medicine 2007; 48: 039-042.

[21] Polster BM, Fiskum G. Mitochondrial mechanisms of neural cell apoptosis. J Neurochem 2004; 90: 1281-1289.

[22] Chua BT, Volbracht C, Tan KO, Li R, Yu VC, Li P. Mitochondrial translocation of cofilin is an early step in apoptosis induction. Nat Cell Biol 2003; 5: 1083-1089.

[23] Cheng EH, Wei MC, Weiler S, Flavell RA, Mak TW, Lindsten T, Korsmeyer SJ. BCL-2, BCL-X L sequester BH3 domain-only molecules preventing BAX-and BAK-mediated mitochondrial apoptosis. Mol Cell 2001; 8: 705-711.

[24] Antonsson B, Montessuit S, Sanchez B, Martinou JC. Bax is present as a high molecular weight oligomer/complex in the mitochondrial membrane of apoptotic cells. J Biol Chem 2001; 276: 11615-11623.

[25] Fan T, Lu H, Hu H, Shi L, McClarty GA, Nance DM, Greenberg AH, Zhong G. Inhibition of apoptosis in chlamydia-infected cells: blockade of mitochondrial cytochrome c release and caspase activation. J Exp Med 1998; 187: 487-496.

[26] Hormozi-Nezhad MR, Bagheri H, Bohloul A, et al. Highly sensitive turn-on fluorescent detection of captopril based on energy transfer between fluorescein isothiocyanate and gold nanoparticles. J Lumin 2013; 134: 874-879.